Int. J. Multiphase Flow Vol. 7, No. 6, pp. 563–580, 1981
Printed in Great Britain.

0301-9322/81/060563-18$02.00/0
Pergamon/Elsevier

FLOW REGIMES AND FLOW TRANSITIONS IN LIQUID FLUIDIZED BEDS

ANJANI K. DIDWANIA and G. M. HOMSY

Department of Chemical Engineering, Stanford University, Stanford, CA 94305, U.S.A.

(*Received* 28 *July* 1980; *in revised form* 23 *March* 1981)

Abstract—Using two-dimensional liquid fluidized beds of glass particles in water, we have been able to identify at least four discrete flow regimes. The points of transition between these regimes are sharp and non-hysteretic. The regimes include (in the order of increasing u/u_{mf}), wavy flow, wavy flow with transverse structure, fine-scale turbulent flow, and bubbling states. Characterization of each of these regimes is given in terms of the time and length scales of the motion, as measured by light transmission, optical scanning, and digital time-series analysis. Features of the mechanics of these states are discussed. Observation of the bubbling state for particles of moderate density ($\rho_s = 3990\ \text{kg/m}^3$) in liquid beds is new, and is shown to be related to anomalous expansion data reported by earlier investigators.

1. INTRODUCTION

The occurrence of voidage nonuniformities in liquid fluidized beds is well-known and has aroused considerable theoretical interest in the last two decades. Careful experimental investigation of these nonuniformities has been rather limited and largely motivated by earlier theoretical considerations. Jackson (1963), Pigford & Baron (1965), Anderson & Jackson (1968) and others used the two-fluid continuum equations of motion for fluidized beds to analyze the linear stability of the state of uniform fluidization. Analysis showed that the state was always unstable to small voidage disturbances. Among other things, the growth rate of the disturbances in liquid–solid systems was predicted to be an order of magnitude smaller than that for gas–solid systems. The growth and propagation properties of these voidage disturbances, also referred to as instability voidage waves, were described by linear stability theory. Thus, any theoretical interpretation of experimental results is limited by the usual restrictions which apply to linear theory.

In order to find quantitative support for the theory and to perhaps positively link the voidage waves to the formation of bubbles, experiments were performed in narrow two dimensional liquid fluidized beds by Anderson & Jackson (1969) and El-Kaissy & Homsy (1976). El-Kaissy & Homsy (1976) observed that, after the initial region of exponential growth, the wave train broke down into high voidage clusters which had structures suggestive of bubbles. They obtained statistically significant measurements of the growth and propagation characteristics of the voidage nonuniformities before breakup. These quantitative measurements were later used to deduce values of material constants appearing in the modelling equations. The deduced material constant values were found to be both internally consistent and of reasonable magnitude (Homsy *et al.* 1980). However, the mechanism by which the wave train lost its stability is still entirely unknown.

The results of these experiments were limited in scope to the extent that the experiments were performed in a narrow bed and only over a limited range of fluidization. A host of important questions concerning the nature of voidage fluctuations remains to be investigated. How are the voidage fluctuations related to the properties of fluid and solid, and to the magnitude of the flow? Are the associated particle motions organized at higher fluidization velocity? How fast do the fluctuations occur (time scales of motion)? What are the continuum length scales of the motion (the distances over which the particle motions are correlated)? Are the structure and dynamics of voidage nonuniformities distinct in different flow regimes? Quantitative answers to these questions will help us (a) to discover the scaling laws for the statistical properties of particle motion, (b) to identify flow regimes and the transition points, (c)

to elucidate mechanisms for flow transition, and finally (d) to provide a test of the two fluid continuum theory in terms of its ability to describe experimental results.

Fluidization regimes are currently classified largely on the basis of the macroscopic bed behavior, e.g. bed expansion data or the overall pressure drop across the bed. Smooth bed expansion is identified as particulate fluidization. Aggregative fluidization is marked by the onset of bed height or pressure drop oscillations. Empirical correlations have been developed to relate the bed height to fluidization velocity. Several semiempirical criteria are available to predict (with limited success) the transition point between these two regimes (Wilhelm & Kwauk 1948), Harrison *et al.* 1961, Verloop & Heertjes 1974). Richardson (1971) presents a review of some of these results. Reliance on macroscopic behavior fails to provide any fundamental understanding of the fluid-particle interaction force and has rather limited prospect for scaleup and design purposes. Thus, this approach is far from satisfactory.

Several recent studies have addressed the importance of flow regimes in determining the nature of the motion of gas fluidized beds and in developing good models describing their use as chemical reactors. It is observed that a variety of fluidization behavior including bubble-flow, slug-flow, "apparent" slug flow, turbulent, and "fast" fluidization can occur depending upon the external conditions (see Canada *et al.* 1978, Lanneau 1960, Yerushalmi *et al.* 1978 for a partial discussion. The boundaries between these regimes and the physical mechanisms which lead to transitions from one to the other are at present poorly understood.

The present experimental work on liquid fluidized beds has been motivated by some of the questions raised earlier. Our objective is (a) to identify the various fluidization regimes and the transition points between them using flow visualizations and local voidage fluctuation measurements and (b) to obtain quantitative information on the continuum length and time scales of particle motion, using time series analysis techniques. Our experimental results, described below, report the existence of newly observed fluidization regimes in liquid fluidized beds and have successfully identified the sharp transition points between these flow regimes.

Section 2 briefly describes the experimental apparatus. Flow visualizations and bed expansion data are discussed in section 3. The results of our quantitative measurements are presented in section 4. A discussion of the main features of the results and possible mecahnisms for flow transition is covered in section 5.

2. APPARATUS

Experiments were carried out in a Plexiglass column of 30- × 3.15-cm cross-section and 180 cm high. Figure 1 shows a schematic of the apparatus. The fluidization system used was glass beads in water. A 1.5-kW pump was used to circulate the water in a closed loop from a

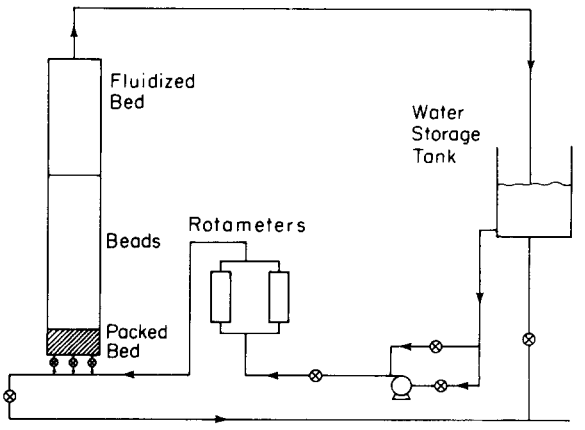

Figure 1. Schematic of the apparatus.

Table 1. Properties of glass beads

Set No.	Code	Diameter cm	Dominant Diameter, d_p cm	Density, ρ_s kg/m
A	304 Class C (Ballotine No. 5)	.0589 - .0417	.059	3990
B	-16 +18 mesh Class VC	.119 - .100	.11	3990
C	-50 +60 mesh Class VB	.0297 - .0250	.029	2990

**Microbeads Division, Cataphote Corporation, Jackson, Mississippi 39205.

holdup tank through a pair of Dwyer Rotameters (Rotameter models RMC-143-SSV-PF and RMC-145-SSV-PF). All piping was 2.54 cm PVC schedule 40.

Flow uniformity was ensured near the base of the bed for the entire range of steady operating conditions. Large scale circulation patterns are known to develop, even in liquid fluidized beds, when the pressure drop across the distributor is small compared with that across the bed itself (Agarwal *et al.* 1980). In case of narrow beds, sintered bronze porous plates, which provide large pressure drop when used as bed support, eliminate flow maldistribution (El-Kaissy 1975). But in wide beds, as in our experiment, porous plates are rapidly clogged causing flow maldistribution and at times, undesirably high pressure drop. Thus for wide beds, an alternate design of distributor section is necessary. We find that a 30-cm high packed bed section filled with glass beads (0.059 cm diameter) and a set of fine wire screens provides uniform flow distribution at the base of the bed and eliminates large scale nonuniformities by maintaining sufficient pressure drop across the distributor.

The experimentally determined values of voidage, superficial fluidization velocity and bed height at minimum fluidization conditions and the ratio of bed thickness to particle diameter for all the cases investigated, are presented in Table 2. The range of fluidization investigated for each case is also included. Such a wide range of fluidization allows a variety of complex behavior.

3. FLOW VISUALIZATIONS

Extensive flow visualizations of the various fluidization regimes were carried out using 35-mm still photography and video tape recording. The bed was backlit with two 500-W flood lamps, with a diffuser screen placed between the bed and lamps. Voidage variations of a few tenths of a per cent were visible to the unaided eye. Figure 2 shows a series of 35-mm still pictures of the bed, under steady operating conditions, in the order of increasing fluidization velocity. We shall discuss the visualizations for the beads of Set A in detail, and only comment on those aspects of the behavior of Sets B and C which differ from those of Set A.

Table 2. Experimental conditions

Set No.	ϵ_{mf}	H_{mf} cm	U_{mf} cm/s	ρ_s/ρ_F	D/d_p	Range of U_s/U_{smf}
A	.37	59.5	.73	3.99	53	$1.0 \leq U/U_{mf} \leq 8.0$
B	.383	42.2	2.05	3.99	29	$1.0 \leq U/U_{mf} \leq 4.0$
C	.358	21.5	.163	2.99	109	$1.0 \leq U/U_{mf} \leq 18.0$

Set A

Over a relatively wide range, $1.0 \leq u/u_{mf} \leq 3.4$, we observed voidage fluctuations in the form of waves travelling upwards in the bed. These are analogous to those reported by El-Kaissy & Homsy (1976). It is useful to note that the organization of the wave motion within this regime depends upon the flow rate and distance.

For flow rates slightly above the minimum fluidization (figure 2a, $u/u_{mf} = 1.4$), the voidage waves become observable only in the upper part of the bed. Figure 2(b) ($u/u_{mf} = 1.7$) shows the wave structure at a higher flow rate. The voidage fluctuations have planar wave form and are observable even close to the distributor section. As these instability waves travel upwards, they develop a transverse structure. This is illustrated in figure 2(c) ($u/u_{mf} = 1.9$). With further increase in flow rate, the horizontal wave length decreases and voidage fluctuations become

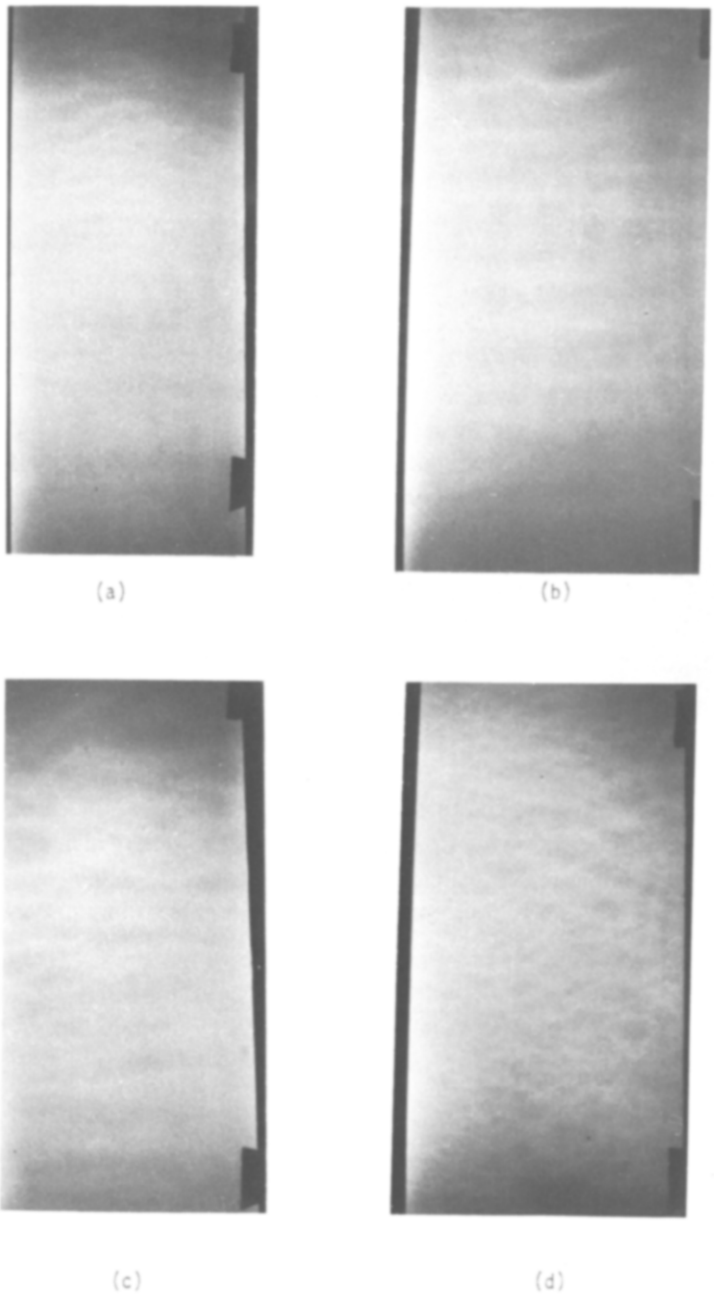

Figure 2(a)–(d).

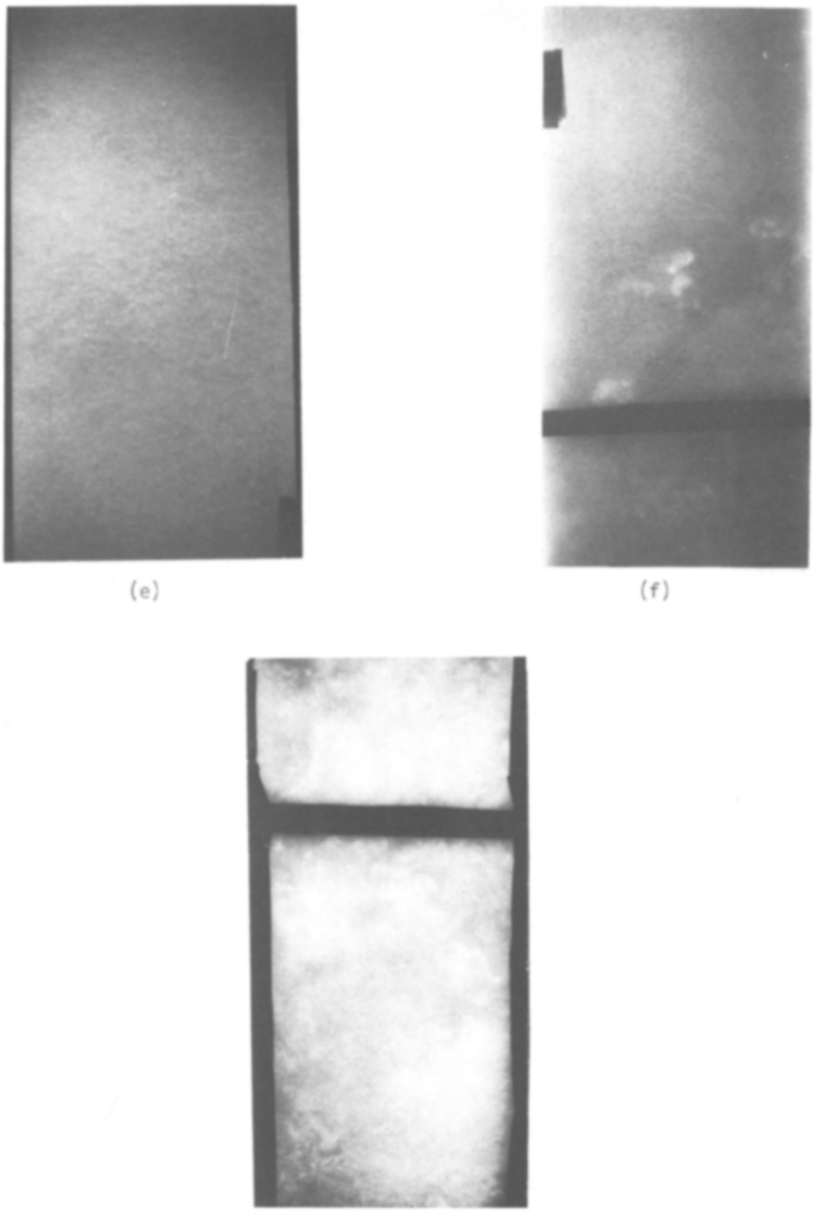

Figure 2. Fluidization regimes in liquid fluidized beds. Wavy regime: (a) $u/u_{mf} = 1.4$, (b) $u/u_{mf} = 1.7$, (c) $u/u_{mf} = 1.9$, (d) $u/u_{mf} = 2.5$. Turbulent regime: (e) $u/u_{mf} = 3.5$, (f) $u/u_{mf} = 4.7$. Bubbly regime: (g) $u/u_{mf} = 6.5$.

increasingly wavy, as evident in figure 2(d) ($u/u_{mf} = 2.5$). Thus, in a wide bed, the wave regime is more complex than we had previously observed, and is characterized by a complicated horizontal structure.

Beyond $u/u_{mf} = 3.4$, the wavy voidage fluctuations disappear. The whole fluidized suspension becomes homogeneous in structure and individual particles execute random motion about some mean position. As before, there is no tendency for bulk circulation of the particulate phase. Figure 2(e) ($u/u_{mf} = 3.5$) is a still picture of this turbulent fluidization regime. There is no preferential continuum length scale over which the particle motion is organized. As seen in figure 2(f) ($u/u_{mf} = 4.7$), for $u/u_{mf} \geq 4.4$, patches of high voidage regions appear sporadically. Using techniques described below, we estimate $\epsilon = 0.87$ for these regions.

These bubbles are 2–3 cm in diameter and they travel upwards in the bed. The background is still in the turbulent fluidization regime.

A sudden transition from the turbulent regime to a bubbly regime takes place at $u/u_{mf} = 6.5$. Strong interactions and the propagation characteristics of bubbles in this regime are highly unsteady, thus leading to complicated bubble dynamics. Figure 2(g) ($u/u_{mf} = 6.5$) gives an instantaneous view of this bubbly state.

Set B

For this set of particles, the range of fluidization investigated was $1.0 \leq u/u_{mf} \leq 4.0$. The wavy regime, similar to the one described above, was observed over the range $1.0 \leq u/u_{mf} \leq 2.2$. The amplitude of voidage fluctuations was much larger than before. (This was also confirmed by our quantitative measurements to be described later.) The transition to the bubbly regime could not be observed because of the limited range of u/u_{mf} investigated. This restriction arises from the fact that u_{mf} becomes much higher as the particle size increases and our pump had limited capacity.

Set C

A wide range of fluidization was investigated ($1.0 \leq u/u_{mf} \leq 18.0$) for these relatively small particles. Flow visualizations could not be obtained in the range $1.0 \leq u/u_{mf} \leq 6.0$. The intensity of transmitted light through the bed was very low because of high bed depth to particle diameter ratio ($D/d_p = 109$). In addition, the amplitude of the voidage fluctuation in the wavy regime was very small. This amplitude is approximately proportional to d_p^3 (see El-Kaissy & Homsy 1976). Thus, the transition point between the wavy and the turbulent regime could not be observed directly in this apparatus.

The results of our flow visualizations are summarized in a flow transition diagram shown in figure 3. We note that even though the nature of the bed expansion indicates what is usually called "particulate" fluidization, there exist a number of different regimes, some of which are reported here for the first time. For Set A, at $u/u_{mf} = 1.0$, the packed bed becomes fluidized. In the wavy regime, for $1.0 \leq u/u_{mf} \leq 3.4$, well-organized instability voidage waves are observed. A new turbulent flow regime is observed over the range $3.4 \leq u/u_{mf} \leq 6.5$, with occasional bubbles

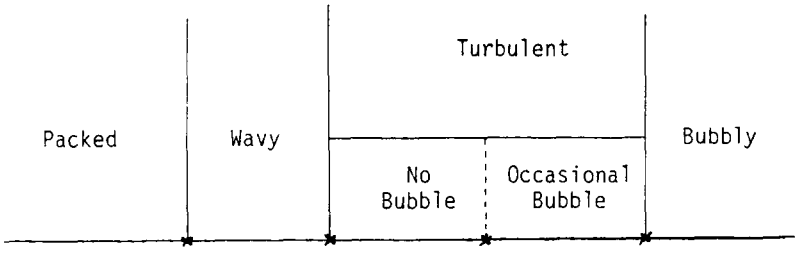

	$u/u_{mf} \longrightarrow$				$Ga \times 10^{-4}$
Set A	1.0	3.4	4.4	6.5	2.0
Set B	1.0	2.2	3.5	*	13.0
Set C	1.0	*	10.0	11.5	0.24

*Not observed due to limitations imposed by experimental setup.

Figure 3. Flow transition diagram.

appearing for $u/u_{mf} \geq 4.4$. Beyond $u/u_{mf} = 6.5$, a bubbling flow regime appears. Such a bubbling regime in liquid fluidized beds has been reported earlier only for a high ratio of solid to fluid density, e.g. the lead shot-water system (Davidson & Harrison 1963). The transition points between these flow regimes in all three cases are observed to be well defined, sharp and do not exhibit hysteresis, i.e. their values do not depend on whether the fluid flow is being increased or decreased. As seen in figure 3, the transitions for Sets B and C are similar in nature, but the specific transition points change.

The macroscopic behavior of the bed is also of interest, and can be monitored by obtaining bed expansion data. In both the wavy and turbulent regimes, the bed expansion is smooth, but fluctuations in bed height are observed in the bubbly regime. Figures 4–6 show Richardson–Zaki plots of the dimensionless fluidization velocity vs time averages mean voidage, ϵ_0 for the three

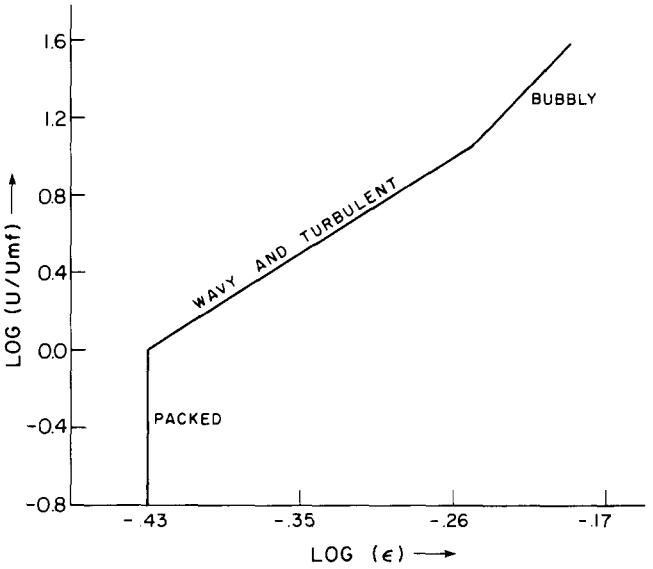

Figure 4. Bed expansion for Set A.

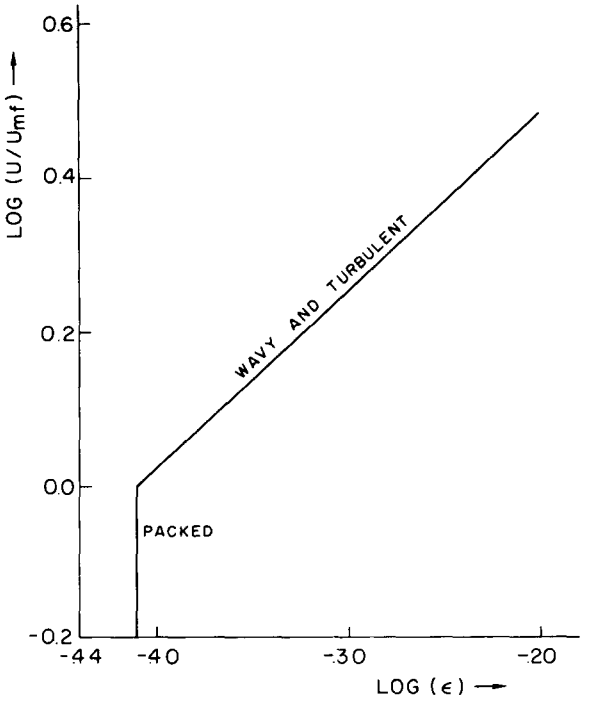

Figure 5. Bed expansion for Set B.

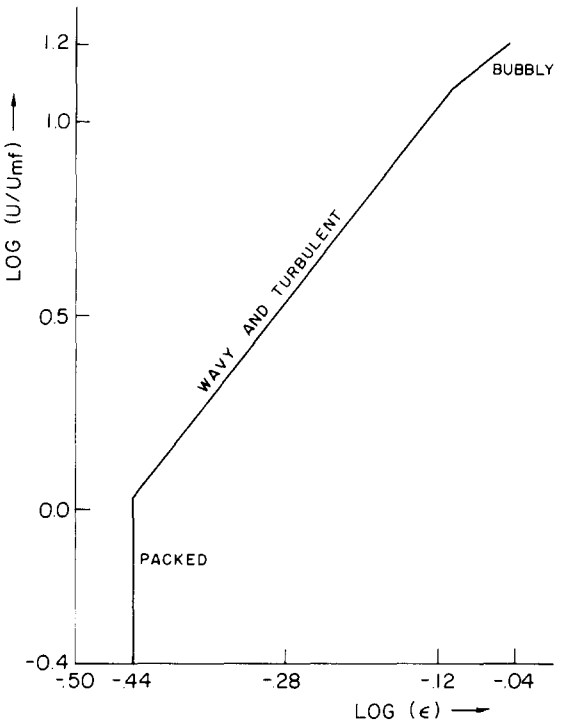

Figure 6. Bed expansion for Set C.

sets. For Sets A and C, we observe a discontinuity in bed expansion, similar to one noted by Couderc & Riba (1977). In both cases, the appearance of this discontinuity coincides with the transition point between the turbulent and bubbling regimes. We also notice that the bed expansion data cannot be used to distinguish between the wavy and the turbulent regime.

4. QUANTITATIVE MEASUREMENTS

As our flow visualizations illustrate, the nature of voidage fluctuations differ in these various flow regimes. Thus we would expect the statistical properties of these fluctuations, i.e. the relevant time and length scales, to vary widely over the range of fluidization velocities for each set of particles investigated.

To obtain quantitative information about these statistical properties, we use light transmission techniques, which utilize the observation that for a bed uniformly illuminated from behind, the transmitted light intensity is linearly proportional to the local voidage (El-Kaissy 1975). This linear relation allows us to deduce the relevant time and length scales of voidage fluctuations from the spatial and temporal variation of the transmitted light intensity.

The two techniques that we used for recording these fluctuations in the light intensity are: (a) a two-point correlation technique and (b) an optical scanning technique. In the former, we record and analyze the time history of voidage fluctuations at any two points in the bed simultaneously along the mean fluid flow direction. This technique yields the amplitude and the frequency content of local voidage fluctuations as well as their velocity of propagation. However, since we are using only two point probes, the two-point correlation technique fails to provide any information about the transverse structure of these voidage waves and is suitable for analyzing only the local time variation of the fluctuations. To obtain quantitative information about the transverse structure of these voidage waves, we need to take another approach. We developed a new optical technique to analyze the spatial voidage variations and thus obtain the relevant length scales. In this optical technique, we store the instantaneous transmitted light intensity in each of two dimensions on a photographic film and later convert the spatial variation in light intensity to a time varying signal for analysis purposes. Below, we

discuss the details of each of these techniques, the data acquisition system, and the statistical analysis techniques used. We also present the quantitative results, for each set of particles, obtained using each of these techniques.

In the two-point correlation technique, the transmitted light was measured by two UDT (United Detector Technology) photop 450 (photodiode/amplifier combination). The photops are light-to-voltage converter solid state devices. They combine a high reliability PIN Silicone Photodiode and a low noise current mode operational amplifier in the same package. They are highly light sensitive and possess a linear response over a wide range of signal levels. The photodiode box was identical to that used by El-Kaissy & Homsy (1976). An aperture size of ~0.7 cm was found to be suitable for measuring continuum motions without losing the resolution of motions on the length scales of the waves, and the distance between the photops was known. The d.c. component of the signal from the photops was separated and monitored by a Fluke 8000A digital multimeter. The d.c. level was linearly related to the mean voidage level and was found to remain constant over a period of 5 min. The a.c. component of the signal was analyzed by the data acquisition and analysis system to be described below.

In the optical scanning technique, the instantaneous transmitted light through the bed in two dimensions is stored on a photographic film. Thus, the transmittance of the film, when uniformly illuminated, is linearly proportional to local voidage fluctuations. The transmitted light intensity variations are sensed by a miniature array of precisely aligned photodiodes. This miniature array—a high density monolithic silicon integrated circuit—is manufactured by EG & G Reticon. The particular device type that we used was RL-1024G photodiode array with RC303 current amplifier circuit and RC100A sample-and-hold circuit. It has a long narrow rectangular apertured light sensing region in an opaque mask. The entire aperture is composed of a linear array of 1024 light sensitive photodiodes. The aperture length is 2.5 cm and width 26 μm, thus providing very high spatial resolution. It was held against the photographic film, along the line we wish to scan, with a uniform light source on the other side. The photodiodes scanned the line at a rapid rate (the exposure time for each photodiode element is 4 μs) and produced a series of charge-pulses corresponding to the pattern of light intensity to produce an electrical analog of this image. This signal was fed to a sample-and-hold electronic interface, whose output could be conveniently sampled by our data acquisition system.

The signal from the photops and also the reticon signal from the sample-and-hold circuit were analyzed by a Digital Equipment Corp. PDP 11/34 (host processor unit) and PDP 11/03 (remote processor unit) minicomputer system. Signals were simultaneously digitized and recorded on a Brush 220 chart recorder. The chosen sampling rate (50 Hz) was well beyond the Nyquist frequency. All of the sampled data were then sent to the storage disk on the host unit for later analysis.

The discretized data were analyzed using time series analysis techniques. For the two-point correlation technique, the typical frequency resolution was 0.097 Hz, and for the optical scanning technique, the spatial resolution was 0.025 cm. A detailed description of the signal flow charts is given in Didwania (1981).

We discuss the analysis in detail for Set A. The measurements for Sets B and C were similar, and only the final results are given in table 4. Figure 7 shows typical traces obtained in the different flow regimes at a fixed height of 35 cm above the distributor along the centerline of the bed. The dual traces at each flow rate correspond to the simultaneous outputs of the two photops, with the top trace corresponding to the top photop. In figure 7(a) ($u/u_{mf} = 1.7$), we observe quasiperiodic signal corresponding to coherent planar voidage waves travelling upwards. The time lag between the two signals can be seen clearly. A more complex signal is observed in figure 7(b) ($u/u_{mf} = 2.5$), indicating that the waves no longer have a coherent planar structure. The traces show the presence of increasingly faster voidage fluctuation components. These faster fluctuations relate to decreasing vertical wavelength, increasing transverse structure and loss of phase coherence in the horizontal direction. The traces in figure 7(c) correspond

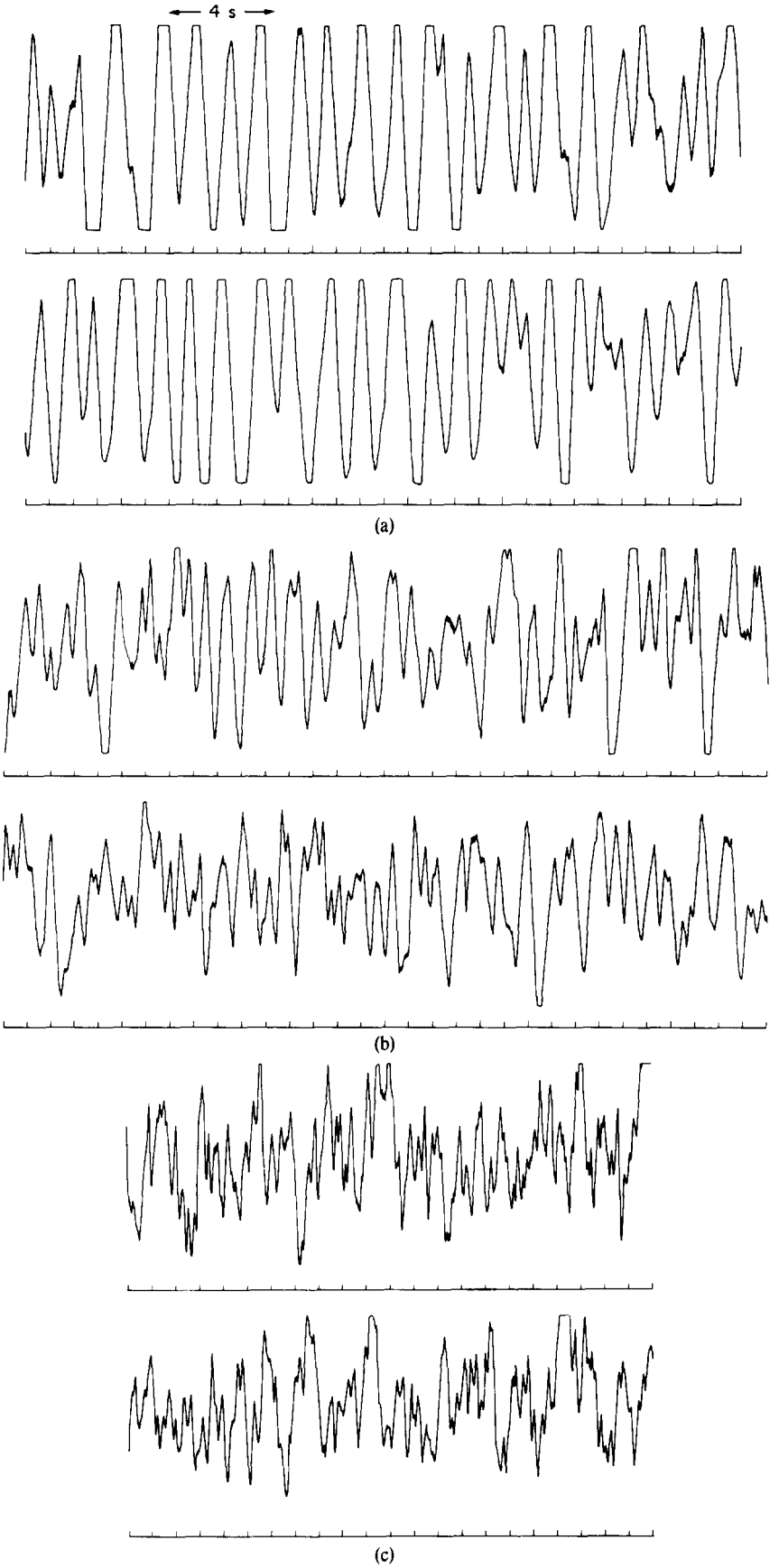

Figure 7(a)–(c).

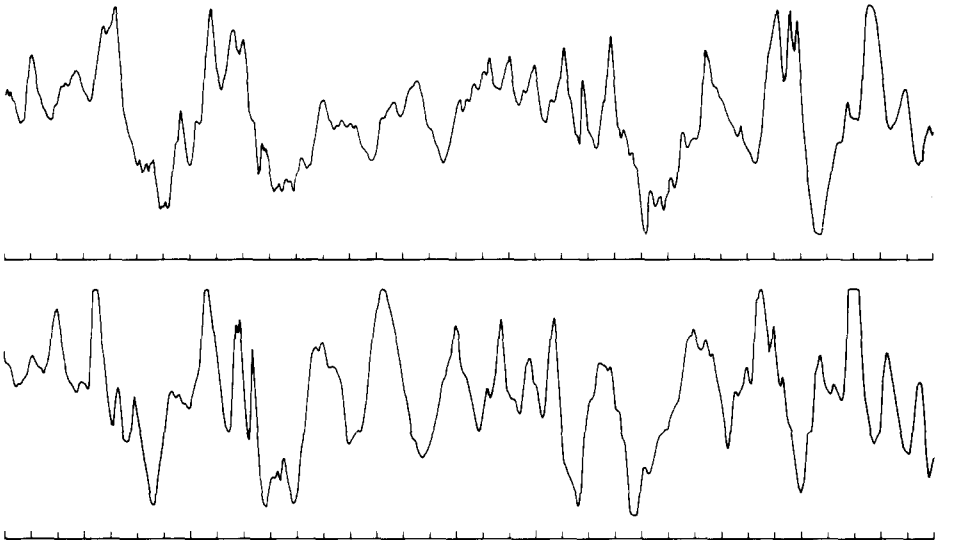

(d)

Figure 7. Sample voidage fluctuation traces in different flow regimes. (a) Planar voidage waves $u/u_{mf} = 1.7$. (b) Waves with transverse structure $u/u_{mf} = 2.5$. (c) Turbulent fluidization regime $u/u_{mf} = 3.5$. (d) Bubbly regime $u/u_{mf} = 6.5$.

to voidage fluctuations in the turbulent regime. The signals from the two photops are uncorrelated and show loss of periodicity. Figure 7(d) illustrates the voidage fluctuations in the bubbly fluidization regime. The large peaks in the signal correspond to the bubbles passing by the probe. In some cases there is a reasonable correlation between the records, indicating that the bubbles pass both probes vertically and are intact. However, bubble coalescence and sidewide movement of the bubbles are the more common events, and lead to a low overall correlation between the two records. As is well known, some type of conditional sampling is necessary to obtain bubble properties from records such as these (Burgess & Calderbank 1975). This was not done in the present study. The arrival times of the bubbles are random, and the non-stationary nature of the flow is also evident from the traces.

Typical correlations and power spectra of the voidage fluctuations in the wavy and turbulent regimes are shown in figures 8–10. For the planar voidage waves, the autocorrelation function shows a high degree of periodicity (figure 8a). Increasing loss of periodicity is observed at higher flow rates, as seen in figure 8(b) ($u/u_{mf} = 2.5$). In the turbulent regime, the autocorrelation (figure 8c) decays rapidly with a few very small amplitude oscillations, implying that the voidage fluctuations are uncorrelated.

Figure 9 shows, for different flow regimes, the power spectra of the signals, ensemble averaged over fifteen time-records. In the planar wave regime (figure 9a), a narrow spectral peak at approx. 1.5 Hz is readily apparent. This is directly comparable to the frequency reported earlier and measured in a narrow bed (see El-Kaissy & Homsy 1976, figure 9). For waves with transverse structure, the spectral content is more complex, as shown in figure 9(b). It is characterized by a dominant peak at 2.2 Hz. Furthermore, the spectral content of the background extends to over 4.0 Hz. Finally in the turbulent regime (figure 9c) is broad 0.6–6.0 Hz, and flat, an indication of the random nature of the fluctuations.

A typical cross-correlation of the signals, obtained from the two photops, in the planar voidage regime is shown in figure 10. It has a distinct peak and shows periodicity. The periodicity and the time delay corresponding to the peak yield the vertical wavelength and the velocity of these voidage waves respectively. The propagation velocities of the bubbles in the bubbling regime can be estimated from traces as in figure 7(d).

Some typical results of our quantitative measurements are summarized in table 3. Of particular interest is the amplitude of the voidage fluctuations, which for the bubbly state are

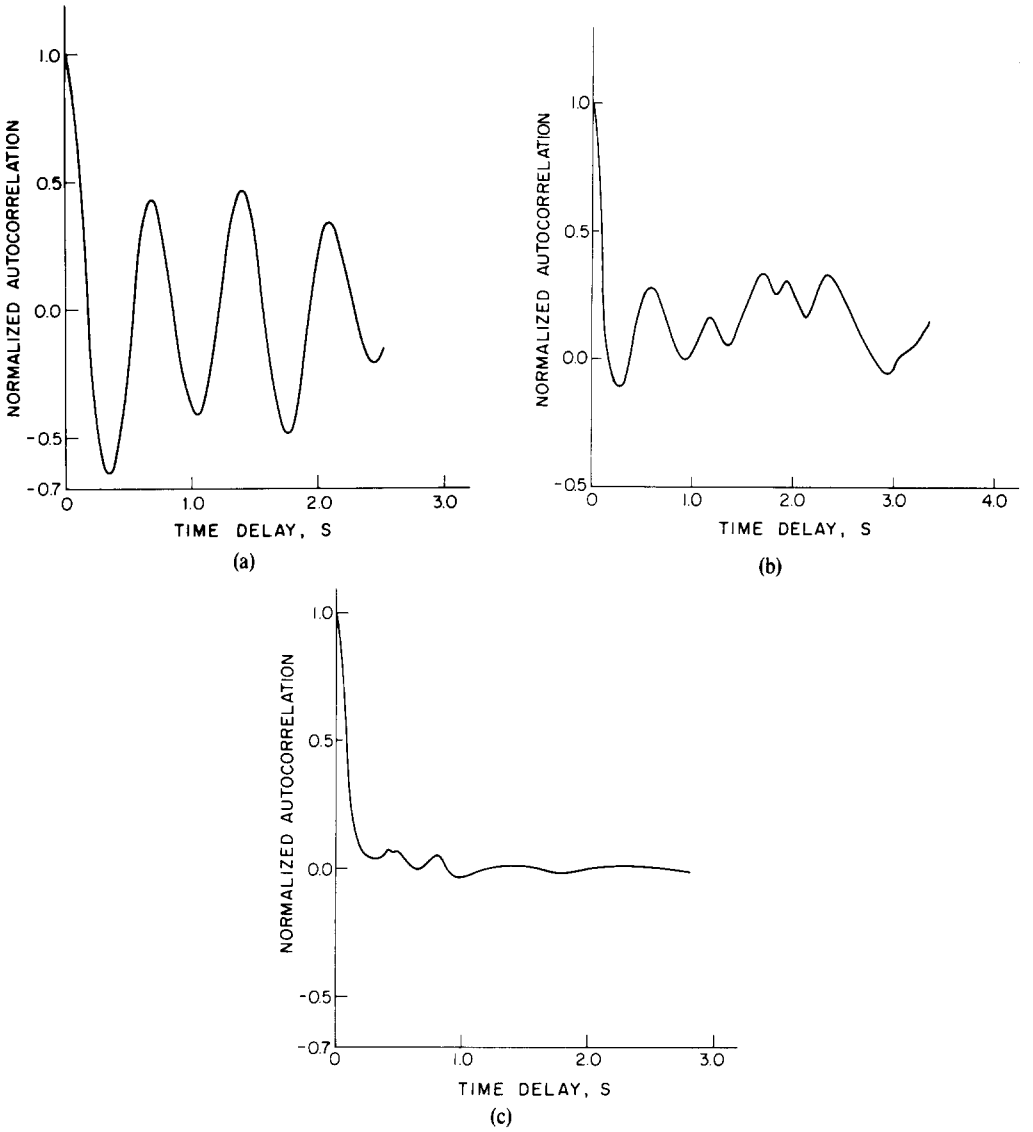

Figure 8. Typical autocorrelations (single realization). (a) Planar voidage waves $u/u_{mf} = 1.7$. (b) Waves with transverse structure $u/u_{mf} = 2.5$. (c) Turbulent regime $u/u_{mf} = 3.5$.

Table 3. Results of quantitative measurements for Set A

Flow Regime		Frequency in Hz	Propagation Velocity in cm/s	Wavelength in cm Horizontal λy Vertical λz	Mean Voidage ε_o	Root Mean Square Voidage Fluctuation ε'
WAVY	Planar Voidage Waves	1.5	5.5	$\lambda y = 30.0$ (wall to wall) $\lambda z = 6.0$	0.419	1.46×10^{-3}
WAVY	Transverse Structure	2.2	6-8[a]	$\lambda y = 6.0$ $\lambda z = 4.0$	0.434	1.16×10^{-3}
TURBULENT		0.6-6.0	Uncorrelated	Homogeneous	0.456	1.37×10^{-3}
BUBBLY		Non-Station-ary	10.5[b]	2-3[b] (diameter)	0.562	0.87[c]

[a] Waves are weakly dispersive.

[b] Results are for a typical single bubble.

[c] Typical bubble voidage.

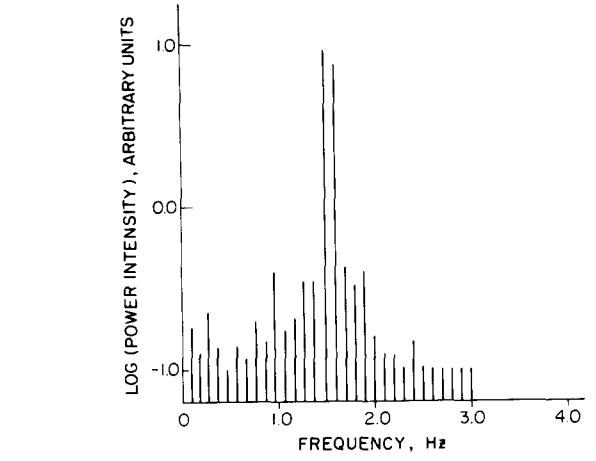

(a)

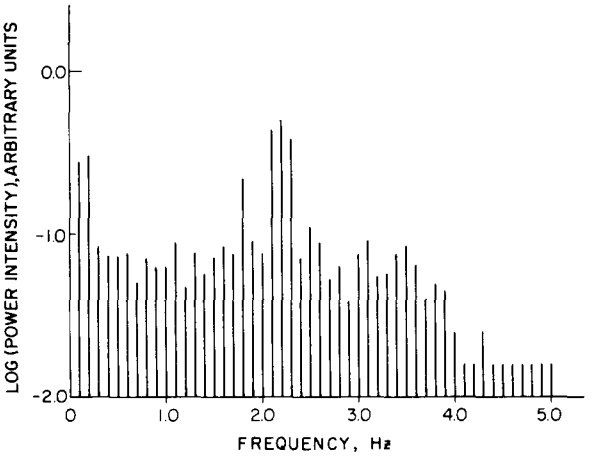

(b)

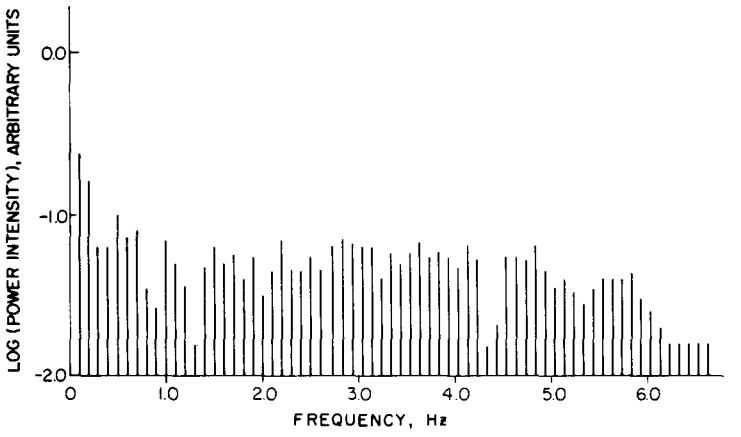

(c)

Figure 9. Typical averaged power spectra. (a) Planar voidage waves $u/u_{mf} = 1.7$. (b) Waves with transverse structure $u/u_{mf} = 2.5$. (c) Turbulent regime $u/u_{mf} = 3.5$.

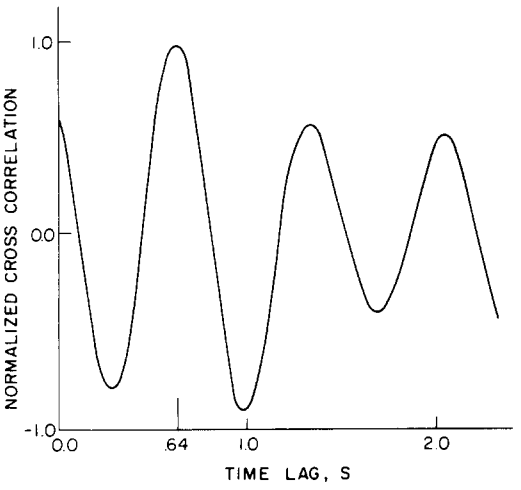

Figure 10. Typical spatial cross correlation for planar voidage waves.

quite large, and for the first three regimes are comparable to those previously observed (El-Kaissy & Homsy 1976, figure 8 and table 5).

Figures 11 and 12 show the power spectra of the signals related to spatial voidage variations in the wavy and the turbulent regime obtained by the optical scanning technique. Figure 11 yields the dominant vertical and horizontal wavelength of the wavy voidage fluctuations. In the turbulent regime, figure 12, we observe that both horizontal and vertical wavelengths are very close. Furthermore, their numerical values verify our visual observation regarding the fine length scale in the turbulent regime.

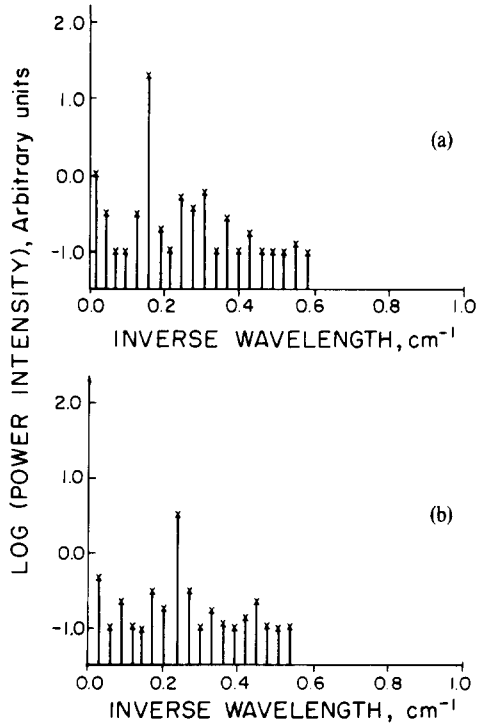

Figure 11. The spatial structure for Set A in the wavy regime, $u/u_{mf} = 2.3$. (a) Horizontal voidage variation. (b) Vertical voidage variation.

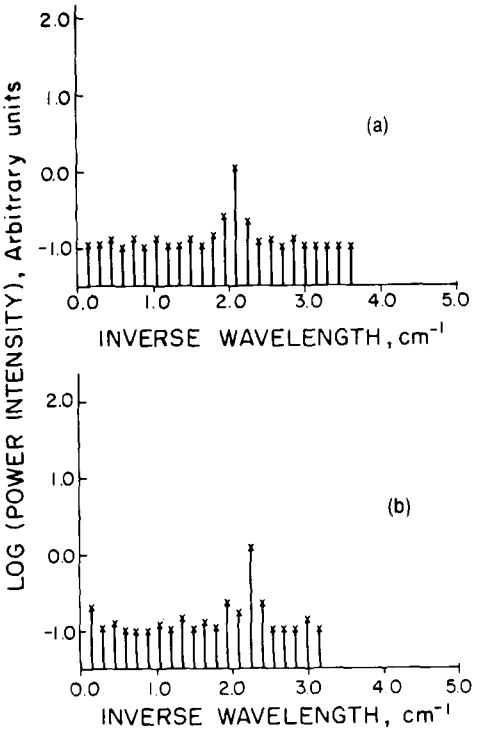

Figure 12. The spatial structure for Set A in the turbulent regime, $u/u_{mf} = 3.5$. (a) Horizontal voidage variation. (b) Vertical voidage variation.

Some typical results of our quantitative measurements are summarized in tables 3 and 4. Of particular interest is the amplitude of the voidage fluctuations, which for the bubbly state are quite large, and for the first three regimes are comparable to those previously observed (El-Kaissy & Homsy 1976, figure 8 and table 5).

5. DISCUSSION

Our studies have shown that the state of motion in a liquid fluidized bed is complex and that the flow has distinct regimes, each of which has characteristic features. The transition points between these regimes are sharp and without hysteresis. The main results of our flow visualizations are summarized in the flow transition diagram (figure 3). The observation of bubbly states in liquid fluidized beds at high flow rates and such low density ratio appears to us to be new. We have also shown that while some flow transitions may be identified by macroscopic bed behavior, such as that from turbulent to bubbly, others may not. Quantitative measurements on the length and time scales of voidage fluctuations in different flow regimes are also reported.

Table 4. Results of quantitative measurements for Set B

Flow Regime		Frequency in Hz	Propagation Velocity in cm/s	Wavelength in cm Horizontal λy Vertical λz	Mean Voidage ε_o	Root Mean Square Voidage Fluctuation ε'
WAVY	Planar Voidage Waves	1.6	4.6	$\lambda y = 30.0$ (wall to wall) $\lambda z = 7.4$	.42	1.71×10^{-2}
	Transverse Structure	2.3	5-6.5[a]	$\lambda y = 6.0$ $\lambda z = 3.0$	.44	1.65×10^{-2}
TURBULENT		0.6-6.5	Uncorrelated	Homogeneous	.51	1.74×10^{-2}

[a] Waves are weakly dispersive.

Elementary dimensional analysis indicates that there are six independent dimensionless groups which describe this two phase system.

$\mathrm{Ga} = gd_p^3/\nu^2$	Galileo number
$\mathrm{Fr} = u^2/gd_p$	particle Froude number
ρ_s/ρ_f	density ratio
L/d_p, D/d_p	bed size, measured in particle diameters
ϵ	void fraction

The choice is not unique. For example, one may use the particle Reynolds number $\mathrm{Re} = ud_p/\nu$ which can be easily expressed in terms of Ga and Fr ($\mathrm{Re} = \sqrt{(\mathrm{Ga} \cdot \mathrm{Fr})}$). For each set of beads four of the above groups (ρ_s/ρ_f, L/d_p, D/d_p and Ga) are fixed at values given in table 2. Wall and entrance effects are negligible because of the high values of L/d_p and D/d_p. Only the Froude number changes with flowrate. Since both u_{mf} and the terminal velocity of a single particle are fixed once Ga, ϵ and ρ_s/ρ_f are given, there is both a lower and upper limit to the range of Froude number that will be observed. We note that the often used and convenient dimensionless group u/u_{mf} can be easily related to the particle Froude number.

Figure 3 shows that the general flow regime behavior remains the same but the values of the parameters at the transition points differ for the three cases studied. We note that Ga number has a strong effect on the transition point values. With increase in Ga, the wavy and turbulent regimes are observed over narrower ranges of fluidization. We also observe that the amplitude of voidage fluctuation is a strong function of particle size. Our observation is not in disagreement with our previous observation that the amplitude increase linearly with Ga number, i.e. as the cube of the particle diameter. We also see that there is a weak particle size effect on the frequency content of the voidage fluctuations.

The relationship of the regimes studied here to those occurring in gas fluidized beds is of some interest. In gas beds of moderate size, the wavy regime is of course absent, and the progression appears to be bubbly → slug → "apparent" slug → turbulent (see Canada *et al.* 1978). The existence of the slug and "apparent" slug regime depends upon the aspect ratio, and there is evidence in large diameter beds for the direct transition from bubbly to turbulent regimes. It is interesting that for the density ratio studied here, the transition is from turbulent to bubbly, i.e. just the opposite. Clearly the progression depends upon density ratio in a crucial way.

A systematic investigation of various physical mechanisms causing flow transition is also of great interest and remains to be studied theoretically in connection with the present quantitative studies. The growth and propagation properties of the planar voidage waves (figure 2b) were satisfactorily accounted for by a linear stability theory (Homsy *et al.* 1980). The dispersion relation for two-dimensional wave propagation predicts that the growth constant is maximum for planar waves. Thus, within the linear theory, we expect the voidage waves to maintain their planar character as they traverse the entire bed height. But our observations are to the contrary. With increase in flow rate or far away from the distributor section these planar waves develop a transverse structure. This suggests that the planar voidage wavetrain itself is unstable and a secondary instability mechanism leads to the appearance of waves with finite horizontal wavelength, and ultimately to the homogeneous turbulent state.

A plausible mechanism for this type of secondary instability, in the framework of a weak nonlinear theory, remains to be examined in detail. Such "near linear" theory has been developed in the context of analyzing the stability of a periodic progressive wavetrain on deep water waves (Stokes waves). It is known that a disturbance capable of gaining energy from the primary wave motion (Stokes waves) consists of a pair of wave modes at side band frequencies and wavenumbers fractionally different from the fundamental frequency and wavenumber.

Such nonlinear interaction appears to be responsible for the appearance of voidage waves with transverse structure. Initial planar voidage waves grow in amplitude as they travel upwards. Once their amplitude becomes appreciable, the nonlinear effects can no longer be neglected. At higher fluidization velocities the nonlinear effects become appreciable at heights closer to the distributor section. As a consequence of non-linearity, these primary planar modes may become unstable to a two-dimensional disturbance composed of a finite number of modes which are capable of resonant interaction with them. Such a secondary instability mechanism can provide a satisfactory explanation of the nature of voidage fluctuations in the wavy regime and is the subject of current work.

Acknowledgement—We wish to thank Dr. David Peri and Prof. J. Goodman for assistance with the optical scanning measurements, and to Prof. J. B. Keller for helpful discussions on nonlinear wave mechanics. Acknowledgement is made to the Donors of the Petroleum Research Fund, administered by the American Chemical Society, for partial support of this research. The continuing support of the Solids and Particulates Processing Program of the NSF is also gratefully acknowledged.

REFERENCES

AGARWAL, G. P., HUDSON, J. L. & JACKSON, R. 1980 Fluid mechanical description of fluidized beds. Experimental investigation of convective instabilities in bounded beds. *Indust. Engng Chem. Fundls* **19**, 59–66.

ANDERSON, T. B. & JACKSON, R. 1968 A fluid mechanical description of fluidized beds—stability of the state of uniform fluidization. *Indust. Engng Chem. Fundls* **7**, 12–21.

ANDERSON, T. B. & JACKSON, R. 1969 A fluid mechanical description of fluidized beds—comparison of theory and experiment. *Indust. Engng Chem. Fundls* **8**, 137–144.

BURGESS, J. M. & CALDERBANK, P. H. 1975 The measurement of bubble properties in two phase dispersions–III. *Chem. Engng Sci.* **30**, 1511–1518.

CANADA, G. S., MCLAUGHLIN, M. H. & STAUB, F. W. 1978 Flow regimes and void fraction distribution in gas fluidization of large particles in beds without tube banks. *AIChE Symp. Ser.* **76**(176), 14–26.

COUDERC, J. P. & RIBA, J. P. 1977 Expansion de couches fluidisees par des liquides. *Can. J. Chem. Engng* **55**, 118–121.

DAVIDSON, J. F. & HARRISON, D. 1963 *Fluidized Particles*. Cambridge Univ. Press, London.

DIDWANIA, A. K. 1981 Voidage instabilities and fluidization regimes in liquid fluidized beds. Ph.D. Thesis, Stanford Univ.

EL-KAISSY, M. M. 1975 The thermomechanics of multiphase systems with applications to fluidized continua. Ph.D. Thesis, Stanford Univ.

EL-KAISSY, M. M. & HOMSY, G. M. 1976 Instability waves and the origin of bubbles in fluidized beds—I Experiments. *Int. J. Multiphase Flow* **2**, 379–395.

HARRISON, D., DAVIDSON, J. F. & DE KOCK, J. W. 1961 On the nature of aggregative and particulate fluidization. *Trans. Instit. Chem. Engrs* **39**, 202–211.

HOMSY, G. M., EL-KAISSY, M. M. & DIDWANIA, A. K. 1980 Instability waves and the origin of bubbles in fluidized beds—II Comparison of theory with experiment. *Int. J. Multiphase Flow* **6**, 305–318.

JACKSON, R. 1963 The mechanics of fluidized beds—I. The stability of the state of uniform fluidization. *Trans. Instit. Chem. Engrs* **41**, 13–21.

LANNEAU, K. P. 1969 Gas–solids contacting in fluidized beds. *Trans. Instit. Chem. Engrs* **38**, 125–143.

PIGFORD, R. L. & BARON T. 1965 Hydrodynamic stability of a fluidized bed. *Indust. Engng Chem. Fundls* **1**, 81–87.

RICHARDSON, J. F. 1971 In *Fluidization* (Edited by J. F. Davidson and D. Harrison). Academic Press, New York.

VERLOOP, J. & HEERTJES, P. M. 1974 On the origin of bubbles in gas fluidized beds. *Chem. Engng Sci.* **29**, 1101–1107.

WILHELM, R. J. & KWAUK, M. 1948 Fluidization of solid particles. *Chem. Engng Prog.* **44**, 201–218.

YERUSHALMI, J., CANKURT, N. T., GELDART, D. & LISS, B. 1978 Flow regimes in vertical gas–solid contact systems. *AIChE Symp. Ser.* **74**(176), 1–13.